Makara Journal of Science

Volume 23
Issue 4 *December*

Article 7

12-20-2019

Impact of El Niño and El Niño Modoki Events on Indonesian Rainfall

Iskhaq Iskandar
Department of Physics, Faculty of Mathematics and Natural Sciences, Universitas Sriwijaya, Palembang 30662, Indonesia, iskhaq@mipa.unsri.ac.id

Deni Okta Lestrai
Graduate School of Environmental Science, Universitas Sriwijaya, Palembang 30139, Indonesia

Muhammad Nur
Department of Physics, Faculty of Mathematics and Natural Sciences, Universitas Sriwijaya, Palembang 30662, Indonesia

Impact of El Niño and El Niño Modoki Events on Indonesian Rainfall

Cover Page Footnote

We thank two anonymous reviewers for their useful and constructive comments. This study is supported by the Ministry of Research, Technology and Higher Education, and the University of Sriwijaya through the research grant Hibah Unggulan Profesi 2019. Ferret software was used for the graphics and analysis.

Makara Journal of Science, 23/4 (2019), 217-222
doi: 10.7454/mss.v23i4.11517

Impact of El Niño and El Niño Modoki Events on Indonesian Rainfall

Iskhaq Iskandar[1*], Deni Okta Lestrai[2], and Muhammad Nur[1]

1. Department of Physics, Faculty of Mathematics and Natural Sciences, Universitas Sriwijaya, Palembang 30662, Indonesia
2. Graduate School of Environmental Science, Universitas Sriwijaya, Palembang 30139, Indonesia

[*]*E-mail: iskhaq@mipa.unsri.ac.id*

Received March 15, 2019 | Accepted October 28, 2019

Abstract

On an interannual time-scale, the Indonesian climate is strongly influenced by the dynamics of Indo-Pacific climate modes. This study aims to investigate the possible impact of different types of El Niño events, namely, typical El Niño and El Niño Modoki, on Indonesian rainfall variability. Seasonal composite analysis was used to evaluate the magnitude and significance level of the influence of El Niño on the rainfall variability over the Indonesian region. Typical El Niño (hereafter El Niño) has a stronger influence on Indonesian rainfall than the El Niño Modoki during boreal autumn in September, October, and November when the events almost reach their peak. Cold sea surface temperature (SST) anomalies were observed in the Indonesian sea and in the western Pacific during El Niño years, while cold SST anomalies covered only the eastern Indonesian sea during El Niño Modoki years. Strong cold SST anomalies during El Niño years led to stronger low-level wind divergence over the Maritime Continent compared with that during El Niño Modoki years. In addition, the Walker circulation during El Niño years revealed a stronger downward motion over the Maritime Continent than that observed during El Niño Modoki years. This stronger downward motion (low-level wind divergence) during El Niño years reduced lower atmospheric water vapor and suppressed atmospheric convection over the Maritime Continent, leading to a significant decrease in rainfall. Similar situations were also observed during El Niño Modoki years but with a much weaker amplitude.

Keywords: El Niño, El Niño Modoki, Maritime Continent, rainfall, sea surface temperature

Introduction

The El Niño-Southern Oscillation (ENSO) is a coupled ocean-atmospheric mode originating in the tropical Pacific Ocean [1]. The warm phase of ENSO, characterized by a cold sea surface temperature (SST) anomaly in the western tropical Pacific Ocean (and a warm anomaly in the eastern tropical Pacific), is called an El Niño event, while the cold phase of ENSO, the conditions of which are opposite those of the warm phase, is called a La Niña event. Previous studies have shown that both El Niño and La Niña events significantly influence Indonesian rainfall. El Niño events have been shown to significantly reduce rainfall over the Maritime Continent, whereas La Niña events cause excess rainfall over the Maritime Continent [2–5].

Recently, a new type of ENSO, namely, ENSO Modoki, has been proposed [6]. The warm phase of ENSO Modoki, which is the so-called El Niño Modoki, is characterized by a cold SST anomaly in the western and eastern tropical Pacific Ocean, with a warm SST anomaly observed in the central Pacific. The pattern is reversed for La Niña Modoki events. Considering its distinct patterns [6–8], previous studies have also suggested that ENSO Modoki has a unique climate impact on surrounding continents [9–11]. El Niño Modoki causes dry conditions in the northern USA and wet conditions in the western USA during boreal winter [12]. Furthermore, during its decaying phase, El Niño Modoki causes an increase in precipitation over South Korea [13]. Another study has proposed that the impact of El Niño Modoki over Southeast Asia is relatively weaker and centered more northward during boreal winter [10].

Given that these two types of El Niño manifest different SST patterns, we hypothesize that they have distinct impacts on the Indonesian climate. Therefore, in this study, we evaluate the possible impacts of typical El Niño and El Niño Modoki events on the Indonesian climate, with emphasis on their impact on the spatiotemporal variability of Indonesian rainfall. This paper is organized as follows: Section 2 describes the

data and methods used in this study; Section 3 presents and discusses the results; and Section 4 summarizes the main findings of this study.

Data and Methods

Material. This study relies on monthly precipitation data from the Global Precipitation Climatology Centre covering a period of January 1901 to December 2013 with uniform latitudinal and longitudinal resolution of 0.5° [14]. Monthly wind fields, sea level pressure, and moisture flux data were obtained from reanalysis conducted by the National Centers for Environmental Prediction–National Center for Atmospheric Research [15]. The data are categorized into 17 pressure levels (mb) with a uniform horizontal resolution of 2.5° and are available from 1948 to the present. SST data come from the National Oceanographic and Atmospheric Administration's Extended Reconstructed Sea Surface Temperature Version 5 (ERSST V5) with a spatial resolution of 2° × 2° and are available from 1854 to the present [16]. This study used all data for only the period from January 1948 to December 2013 for which all data are available.

Methods. The climatological fields for each variable were calculated based on the period from January 1948 to December 2013. Then, the anomalies of all variables were computed by subtracting the climatological fields from the raw data. Classification by season was conducted as follows: boreal summer captures the period of June – July – August (JJA), boreal autumn encompasses the period of September – October – November (SON), boreal winter season captures the period of December – January – February (DJF), while boreal spring denotes the period of March – April – May.

In this study, the Niño3 index and ENSO Modoki Index (EMI) were used to identify typical El Niño and El Niño Modoki events, respectively. The Niño3 index was defined as the SST anomaly averaged in the region bounded by latitude lines 5°N and 5°S and by longitude lines 150°W and 90°W. EMI is calculated as

$$\mathrm{EMI} = [\mathrm{SSTA}]_A - 0.5[\mathrm{SSTA}]_B - [\mathrm{SSTA}]_C \quad (1)$$

where $[\mathrm{SSTA}]_A$, $[\mathrm{SSTA}]_B$, and $[\mathrm{SSTA}]_C$ represent the respective average SST anomalies over the central (165°E – 140°W, 10°S–10°N), eastern (110°W – 70°W, 15°S–15°N), and western tropical Pacific (125°E – 145°E, 10°S – 20°N) (Ashok et. al., 2007). Within the period of study from January 1948 to December 2013, we have identified 8 El Niño and 11 El Niño Modoki events (Table 1). The definition of El Niño Modoki event was based on the criterion in which the event was identified when the amplitude of EMI is below 1.0 of its standard deviation σ for at least three consecutive seasons [6,17].

Table 1. Years of El Niño and El Niño Modoki Events

Event type	Years
El Niño	1951/1952, 1957/958, 1972/973, 1976, 1982/983, 1987/988, 1997/998, 2006/2007
El Niño Modoki	1958/1959, 1963/1964, 1965/1966, 1967/1968, 1977/1978, 1990/1991, 1991/1992, 1994/1995, 2002/2003, 2004/2005, 2009/2010

To evaluate the seasonal impact of each El Niño type, a composite analysis was used in this study. The composite analysis can be presented as [18,19]

$$x_{composite} = \sum_{i=1}^{n} \frac{x_i}{n}, \quad (2)$$

where x indicates the parameter to be composited (e.g., SST, winds, rainfall, velocity potential and divergent winds) and n is the number of events in the composite. In this study, n indicates the number of El Niño and El Niño Modoki events. The significance level of the composite analysis is determined using one-tailed t-test, which is defined as [18,19],

$$t = \frac{x_{composite} - \overline{x}}{\sigma_x / \sqrt{n}}, \quad (3)$$

where $\overline{x}$ is the averaged value of the respective parameter, n is the number of events in the composite, and σ_x is the standard deviation of the time series of the parameter at each grid data. The degree of freedom is defined as $n - 1$. The composite signal is significant if the t signal is larger than the value at the t distribution table for a certain confidence level.

Results and Discussion

Figure 1 shows the composite precipitation anomaly patterns during El Niño and El Niño Modoki years for three different seasons: boreal summer (JJA), boreal autumn (SON), and boreal winter (DJF). These data show the significant reduction in rainfall observed in boreal autumn during both El Niño and El Niño Modoki events. On the basis of these data, the impact from El Niño events was stronger than that from El Niño Modoki events (Figures 1b, e). However, during boreal summer, the impact of El Niño Modoki events was slightly stronger in western Indonesia, whereas El Niño events significantly reduced rainfall in eastern Indonesia (Figures 1a, d). The impacts of both event types were significantly reduced in boreal winter (Figures 1c, f). While most of the Indonesian region experienced a significant rainfall deficit during boreal autumn (Figure 1b), northern Sumatra had significant excess rainfall. This opposite situation may suggest that other mechanisms play a role in regulating rainfall variation

over northern Sumatra. The topic is beyond the scope of this study and will be reported in our future work.

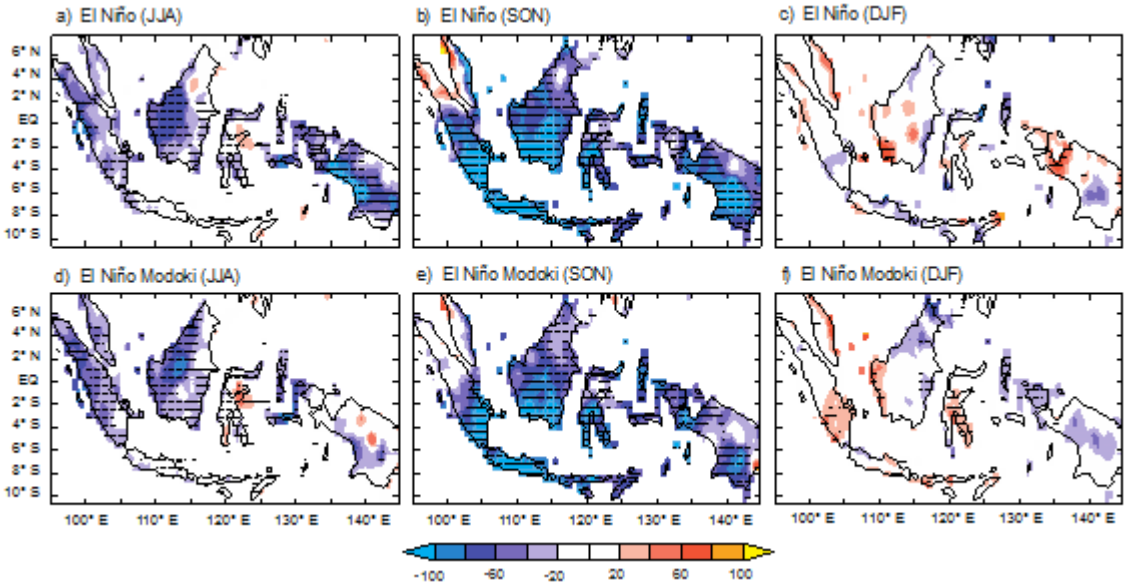

Figure 1. Composite Maps of Rainfall (mm/month) over the Indonesian Region during El Niño (*upper panel*) and El Niño Modoki (*lower panel*) Events in (a,d) Boreal Summer, (b,e) Boreal Autumn, and (c,f) Boreal Winter. Data Points Reaching 90% Confidence are Marked by Cross-hatching

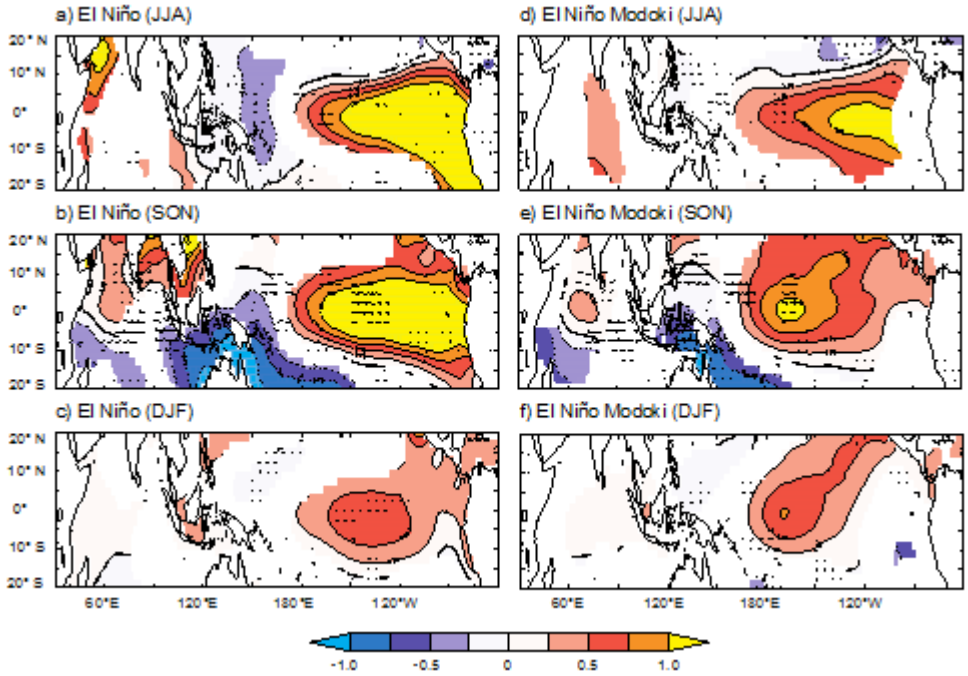

Figure 2. Composite Maps of SST Anomaly (*shaded,* °C) and 850 hPa Winds (*vector,* m/s) during El Niño (*left panel*) and during El Niño Modoki (*right panel*) Years Observed in (a,d) Boreal Summer, (b,e) Boreal Autumn, and (d,f) Boreal Winter. Only Data Points Reaching 90% Confidence Are Shown

To understand the mechanism underlying El Niño's influence on Indonesian rainfall, a composite SST and surface wind anomaly for El Niño and El Niño Modoki years was computed (Figure 2). This composite revealed several different SST anomaly characteristics associated with El Niño and El Niño Modoki events. First, the magnitude of the SST anomaly was weaker during El Niño Modoki than during El Niño events. Second, the location of the warm SST anomaly shifted westward to the central Pacific during El Niño Modoki events. Third, during El Niño years, a stronger and wider negative SST anomaly covered Indonesia and the western tropical

Pacific in boreal autumn (Figure 2b). Meanwhile, during El Niño Modoki events, a negative SST anomaly was observed only in eastern Indonesia (Figure 2e). A strong westerly wind anomaly associated with this SST anomaly gradient was observed over the central equatorial Pacific, while easterly wind anomalies were observed along the southern coast of Sumatra and over the eastern equatorial Indian Ocean.

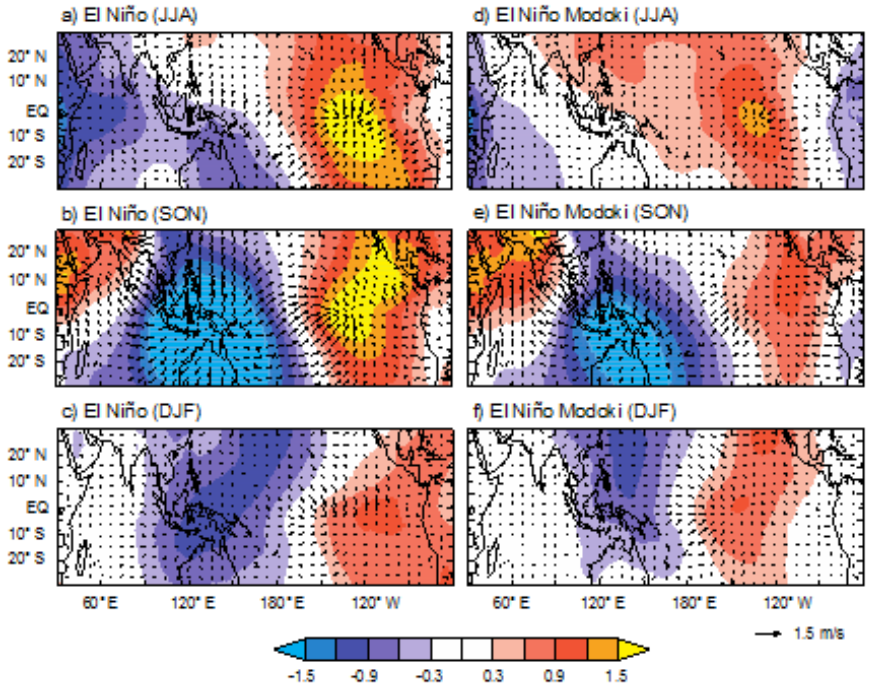

Figure 3. Composite Maps of 850 hPa Velocity Potential (*shaded*, 10^5 m^2/s) and Divergent Winds (*vector*) during El Niño (*left panel*) and during El Niño Modoki (*right panel*) Years Observed in (a,d) Boreal Summer, (b,e) Boreal Autumn, and (d,f) Boreal Winter

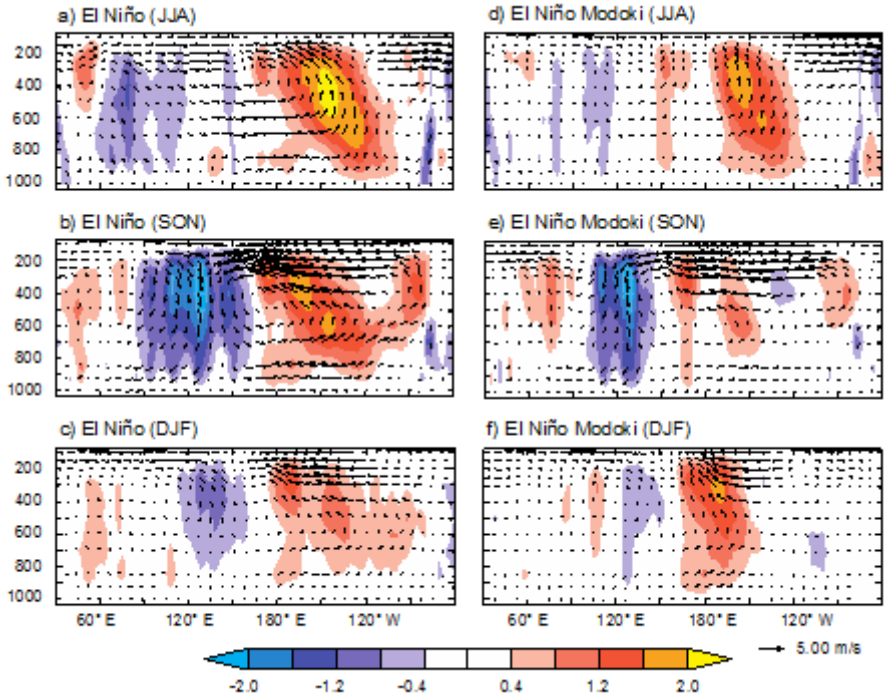

Figure 4. Composite Maps of the Walker Circulation during El Niño (*left panel*) and during El Niño Modoki (*right panel*) Years Observed in (a,d) Boreal Summer, (b,e) Boreal Autumn, and (d,f) Boreal Winter. Only Data Points Reaching 90% Confidence Are Shown

To further examine the distinct mechanisms associated with each El Niño event type, a composite of low-level velocity potential and divergent winds was constructed (Figure 3). A comparison with the composite SST pattern maps revealed that strong divergent winds were collocated with negative SST anomalies, whereas strong convergent winds were collocated with positive SST anomalies (see Figure 2). Given that the gradient of SST anomalies observed during El Niño years was stronger than that observed during El Niño Modoki years, stronger divergent (and convergent) winds were also observed during El Niño years (Figures 3b, e). During El Niño years, a stronger convergent zone in boreal autumn was observed over the Maritime Continent above the coldest SST anomalies, while a stronger divergent zone was observed in the eastern tropical Pacific above the warmest SST anomalies (Figure 3b). The low-level divergent winds were associated with high-level convergent winds, while low-level convergent winds were associated with high-level divergent winds (*not shown*).

Coupled low-level convergent winds and high-level divergent winds were associated with upward Walker circulation motion, while coupled low-level divergent winds and high-level convergent winds were associated with downward Walker circulation motion. Under normal conditions, the Walker circulation is characterized by an upward motion, associated with upper-level westerly winds, in the western Pacific and the Maritime Continent, but by downward motion in the eastern Pacific, associated with low-level easterly winds. The Walker circulation has been suggested to be sensitive to SST variation [1]. To further evaluate the impacts of distinct El Niño event types on Indonesian rainfall, composite maps of the Walker circulation were constructed (Figure 4), in which the Walker circulation was calculated as a zonal-vertical circulation that averaged between 5°S and 5°N.

As expected, during El Niño years, strong downward motions were observed over the Maritime Continent and the western Pacific, while strong upward motions were observed over the central and eastern Pacific during boreal autumn (Figure 4b). Similar patterns were also observed during El Niño Modoki years but with a much weaker amplitude (Figure 4e). Therefore, stronger negative SST anomalies observed within the Indonesian seas and the western equatorial Pacific induced during El Niño years appear to have induced a stronger sea level pressure gradient, leading in turn to stronger low-level westerly wind anomalies along the equatorial Pacific and along the southern coast of Sumatra. These strong low-level westerly winds along the equatorial Pacific were associated with low-level (or high-level) divergent (or convergent) winds, as were easterly winds along the eastern equatorial Indian Ocean and along the southern coast of Sumatra. These wind patterns led to stronger downward motions and suppressed atmospheric convection, thereby resulting in more significant negative rainfall anomalies during El Niño episodes.

Conclusion

In this study, the distinct influences of typical El Niño and El Niño Modoki events on rainfall anomalies over the Indonesian region were evaluated using composite analyses. The results show that the distribution of Indonesian rainfall has different patterns in response to different types of El Niño events. El Niño had a stronger influence than El Niño Modoki on Indonesian rainfall, which reaches its peak during the boreal autumn. Stronger negative SST anomalies in Indonesia and in the western Pacific during El Niño years led to stronger low-level wind divergence over the Maritime Continent and the western Pacific. Low-level divergence and high-level convergence over the Maritime Continent and the western Pacific caused stronger downward motions associated with the western branch of the Walker circulation, thereby suppressing atmospheric convection regionally and leading to more obvious negative rainfall anomalies during El Niño years. A similar situation was observed for El Niño Modoki years but with a much weaker amplitude.

Acknowledgments

We thank two anonymous reviewers for their useful and constructive comments. This study is supported by the Ministry of Research, Technology and Higher Education, and the University of Sriwijaya through the research grant *Hibah Unggulan Profesi 2019*. Ferret software was used for the graphics and analysis.

References

[1] Philander, S. 1989. El Nino, La Nina, and the Southern Oscillation. Academic Press, 46: 293. ISBN 9780125532358.

[2] Nicholls, N. 1984. The Southern Oscillation and Indonesian SST. Mon. Weather Rev. 112: 424–432.

[3] Aldrian, E., Susanto, R.D. 2003. Identification of three dominant rainfall regions within Indonesia and their relationship to sea surface temperature. Int. J. Climatol. 23: 1435–1452, htpp://dx.doi.org/10.1002/joc.950.

[4] Iskandar, I., Utari, P.A., Lestari, D.O., Sari, Q.W., Setiabudidaya, D., Khakim, M.Y.N., Yustian, I., Dahlan, Z. 2017. Evolution of 2015/2016 El Niño and its impact on Indonesia. In AIP Conference Proceedings. Vol. 1857.

[5] Lestari, D.O., Sutriyono, E., Sabaruddin, Iskandar, I. 2018. Severe Drought Event in Indonesia Following 2015/16 El Niño/positive Indian Dipole Events.

J. Phys. Conf. Ser. 1011, htpp://dx.doi.org/10.1088/1742-6596/1011/1/012040.

[6] Ashok, K., Behera, S.K., Rao, S.A., Weng, H. 2007. El Niño Modoki and its possible teleconnection. J. Geophys. Res. 112: 1–27, htpp://dx.doi.org/ 10.1029/2006JC003798.

[7] Kao, H.Y., Yu, J.Y. 2009. Contrasting Eastern-Pacific and Central-Pacific types of ENSO. J. Clim. 22: 615–632, htpp://dx.doi.org/10.1175/2008 JCLI2309.1.

[8] Kug, J.S., Jin, F.F., An, S. 2009. Il Two types of El Niño events: Cold tongue El Niño and warm pool El Niño. J. Clim. 22: 1499–1515, htpp://dx.doi.org/ 10.1175/2008JCLI2624.1.

[9] Weng, H., Ashok, K., Behera, S.K., Rao, S.A., Yamagata, T. 2007. Impacts of recent El Niño Modoki on dry/wet conditions in the Pacific rim during boreal summer. Clim. Dyn. 29: 113–129, htpp://dx.doi.org/10.1007/s00382-007-0234-0.

[10] Feng, J., Wang, L., Chen, W.; Fong, S.K., Leong, K.C. 2010. Different impacts of two types of Pacific Ocean warming on Southeast Asian rainfall during boreal winter. J. Geophys. Res. Atmos. 115: 1–9, htpp://dx.doi.org/10.1029/2010JD014761.

[11] Salimun, E., Tangang, F., Juneng, L., Behera, S.K., Yu, W. 2014. Differential impacts of conventional El Niño versus El Niño Modoki on Malaysian rainfall anomaly during winter monsoon. Int. J. Climatol. 34: 2763–2774, htpp://dx.doi.org/10.1002/ joc.3873.

[12] Weng, H., Behera, S.K., Yamagata, T. 2009. Anomalous winter climate conditions in the Pacific rim during recent El Niño Modoki and El Niño events. Clim. Dyn. 32: 663–674, htpp://dx.doi.org/10.1007/ s00382-008-0394-6.

[13] Kim, S.T., Yu, J., Lu, M. 2012. The distinct behaviors of Pacific and Indian Ocean warm pool properties on seasonal and interannual time scales. J. Geophys. Res. Atmos. 117: 1–12, htpp://dx.doi.org/10.1029/2011JD016557.

[14] Schneider, U., Becker, A., Finger, P., Meyer-christoffer, A., Ziese, M., Rudolf, B. 2014. GPCC's new land surface precipitation climatology based on quality-controlled in situ data and its role in quantifying the global water cycle. Theor. Appl. Clim. 15–40, htpp://dx.doi.org/10.1007/s00704-013-0860-x.

[15] Kalnay, E., Kanamitsu, M., Kistler, R., Collins, W., Deaven, D., Gandin, L., Iredell, M., Saha, S., White, G., Woollen, J.; Zhu, Y.; Chelliah, M.; Ebisuzaki, W.; Higgins, W., Janowiak, J., Mo, K.C., Ropelewski, C., Wang, J., Leetmaa, A., Reynolds, R., Jenne, R., Joseph, D. 1996. The NCEP/NCAR 40-year reanalysis project. Bull. Am. Meteorol. Soc. 77: 437–471.

[16] Huang, B., Thorne, P.W., Smith, T.M., Liu, W., Lawrimore, J., Banzon, V.F., Zhang, H.M., Peterson, T.C., Menne, M. 2016. Full access further exploring and quantifying uncertainties for extended reconstructed sea surface temperature (ERSST) version 4 (v4). J. Clim. 29: 3119–3142, htpp://dx.doi.org/10.1175/JCLI-D-15-0430.1.

[17] Marathe, S., Ashok, K., Swapna, P., Sabin, T.P. 2015. Revisiting El Niño Modokis. Clim. Dyn. 45: 3527–3545, htpp://dx.doi.org/10.1007/s00382-015-2555-8.

[18] Harrison, D.E., Larkin, N.K. 1996. The COADS sea level pressure signal: A near-global El Niño composite and time series view, 1946-1993. J. Clim. 9: 3025–3055.

[19] Yuan, Y., Hongming, Y.A.N. 2013. Different types of La Niña events and different responses of. Chinese Sci. Bull. 58: 406–415, htpp://dx.doi.org/10.1007/s11434-012-5423-5.